Raman Studies on the Self-localized Excitations in Lightly and Heavily Doped *trans*-Polyacetylene with Sodium

Jin-Yeol Kim,*,† Yukio Furukawa,‡ Akira Sakamoto,§ and Mitsuo Tasumi§

Department of Chemistry, College of Natural Science, Hanyang University, Sungdong-Gu, Seoul 133-791, Korea, Department of Chemistry, Faculty of Science and Engineering, Waseda University, Shinjuku-ku, Tokyo 169, Japan, and Department of Chemistry, Faculty of Science, Saitama University, Urawa, Saitama 338, Japan

Received: April 10, 2002; In Final Form: June 28, 2002

The difference of Raman spectra between lightly and heavily Na-doped *trans*-polyacetylene (*trans*-PA) was observed with the 1320 nm laser line, and these were discussed on the basis of the Raman spectra of the negatively charged anions $Ph(CH)_nPh^-$ [DP_n^-, $n = 3$, 5, 7, 9, and 13] and the radical-anion species $Ph(CH)_nPh^{\bullet-}$ [$DP_n^{\bullet-}$, $n = 4$, 6, 8, and 10] and 19,19′,20,20′-tetranor-β,β′-carotene [$TNBC^{\bullet-}$, $n = 22$] of the model compounds, which correspond respectively to negatively charged soliton and negative polarons in *trans*-PA. The observed wavenumbers of the ν_1 and ν_4 bands (C═C and C−C stretches) of lightly doped *trans*-PA are lower than those of the corresponding bands of pristine *trans*-PA, whereas the contrary is the case for heavily doped *trans*-PA. Raman spectra of the negatively charged soliton models (DP_n^-) and the negative polaron models ($DP_n^{\bullet-}$ and $TNBC^{\bullet-}$) were very similar to their spectrum patterns as a whole, but their wavenumbers and relative intensities are mutually different to some extent. In particular, the Raman wavenumbers of heavily doped *trans*-PA are very similar with those of the polaron models. The dispersion of the C═C stretching band (ν_1) in doped PA with the various wavelengths of excitation laser line were explained as the presence of charged domains having various lengths of electron localization.

Introduction

Polyacetylene (PA) [$(CH{=}CH)_n$] is a prototype of conducting polymers.[1,2] This polymer shows high electrical conductivity of more than 10^5 S/cm when chemically doped with electron acceptors (such as iodine, AsF_5, $FeCl_3$, and $HClO_4$) or electron donors (such as alkali metals). The electrical properties of doped PA depend on dopant contents.[3,4] The mechanistic relationship between chemical doping and charge transport in PA has been studied by various physical methods.[5] The pauli spin susceptibility indicative of the metallic density of states appears suddenly at a dopant concentration of about 6 mol %/CH unit (critical value),[4,6] and doped PA can thus be regarded as a metal. When the dopant concentration is below the critical value, charged solitons that have charges but no spin have been proposed as spinless charge carriers.[1] However, a complete understanding of the mechanism of electrical conduction has not yet been achieved, though several arguments have been proposed.

Recently, we have demonstrated the usefulness of resonance Raman spectroscopy in the characterization of self-localized excitations existing in the doped PA.[7−9] The electronic absorption of doped PA is observed in the region from visible to near-infrared. Accordingly, resonance Raman spectroscopy with visible and near-infrared excitations gives structural information on the self-localized excitations. The resonance Raman spectra of a heavily metal-doped PA film and its pristine *trans*-PA excited with laser lines between 363.4 and 1064 nm have shown marked changes with the exciting laser wavelengths.[9−16] The observed frequency dispersion of pristine *trans*-PA has been explained in terms of the existence of segments having various conjugation lengths[7,8] and the effective conjugation coordinate model[9] originating from the amplitude-mode theory. Zerbi et al.[9] have attributed the observed Raman spectra to undoped chains remaining in doped PA, because the intensities of the Raman bands arising from doped domains are expected to be very weak on the basis of their theoretical considerations. In previous papers,[14,15] however, the present authors have attributed the observed Raman bands of Na-doped *trans*-PA to doped domains for the following reasons: (1) The Raman bands of doped domains can be observed because of the resonance enhancement effect, which is not taken into account in the effective conjugation coordinate model. (2) The Raman spectra of heavily Na-doped *trans*-PA are quite similar to those of the charged species of polyenes.[15] (3) A weak Raman band is observed in the range between 1264 and 1254 cm^{-1} for heavily Na-doped *trans*-PA, whereas the corresponding band is observed in the range between 1296 and 1288 cm^{-1} for pristine *trans*-PA. Thus, the presence of a band in the lower wavenumber range (1264−1254 cm^{-1}) is a marker of negatively charged domains. Lefrant et al.[11,16] have also ascribed the observed Raman bands to doped domains. Tanaka et al.[13] have reported the 632.8 nm excited Raman spectra of *trans*-PA doped with Na at various concentrations. However, at dopant concentrations less than about 8 mol %, Raman spectra show no significant changes from those of pristine *trans*-PA. Raman spectra taken with a laser line of wavelength longer than 1064 nm are expected

* To whom correspondence should be addressed. E-mail: jinyeol@hanyang.ac.kr. Phone: 82-2-2281-3214. Fax: 82-2-2281-3236.
† Hanyang University.
‡ Waseda University.
§ Saitama University.

10.1021/jp020948a CCC: $22.00
Published on Web 08/29/2002

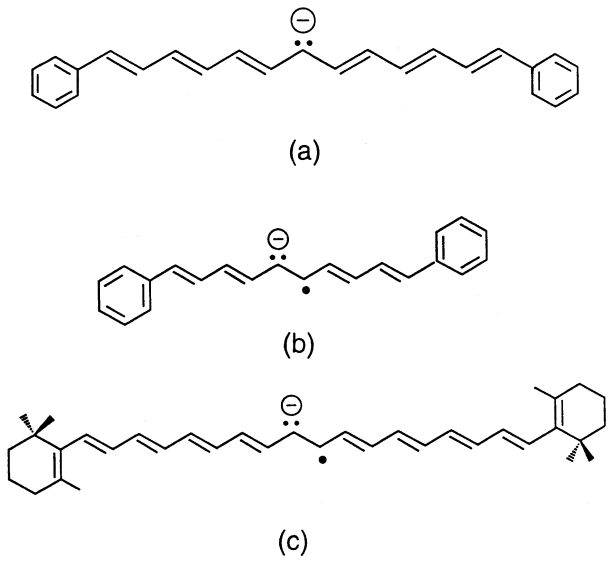

Figure 1. Structures of model compounds: (a) α,ω-diphenylpolyenyl anion [DP_n^-, $n = 13$]; (b) radical anion of α,ω-diphenylpolyene [$DP_n^{\bullet-}$, $n = 10$]; (c) radical anion of 19,19′,20,20′-tetranor-β,β-carotene [$TNBC^{\bullet-}$, $n = 22$]. *n* is the number of carbon atoms in the polyene part.

to be more informative, because the electronic absorption of Na-doped PA appears from visible to infrared.[4,13]

These spectra have been analyzed on the basis of the resonance Raman spectra of the charged species (ions, radical ions, and divalent ions) of conjugated compounds.[17,18] Studies on the charged species of oligo and polyene compounds in particular are not only interesting themselves but also important for understanding the electrical properties of doped *trans*-PA. Charged species of polyenes have been studied as models of doped PA.[19−24] The molecular and electronic structures of the radical cations and dications of 1,3-butadiene to 1,3,5,7,9-decapentaene have been also calculated by an ab initio molecular orbital method at the complete active space self-consistent field (CASSCF) level and using multireference Möller−Plesset theory.[25] Tolbert et al.[19] have reported the NMR and electronic absorption spectra of α,ω-diphenylpolyenyl anions $Ph(CH)_nPh^-$ (abbreviated as DP_n^-, $n = 3$, 5, 7, 9, 13, and 17) as model compounds of a negatively charged soliton in *trans*-PA. In this study, Raman spectra of DP_n^- ($n = 3$, 5, 7, 9, and 13) were observed with the 1064 nm laser line for the first time. These compounds with an odd number of carbon atoms at the polyene parts (*n*) have a negative charge but no spin. The Raman spectra of the radical anion of α,ω-diphenylpolyenes $Ph(CH)_nPh^{\bullet-}$ (abbreviated as $DP_n^{\bullet-}$, $n = 6$ and 8) have been also reported as the model compounds of a negatively charged polaron in *trans*-PA.[15,20] Because the Raman spectra of $DP_n^{\bullet-}$ ($n = 6$, 8) had already been reported,[15] we newly added the experimental part of the present study to $DP_n^{\bullet-}$ ($n = 4$ and 10). In our previous paper,[24] we had also reported the optical absorption and Raman spectra of the radical anion of all-*trans*-19,19′,20,20′-tetranor-β,β-carotene (abbreviated as $TNBC^{\bullet-}$, $n = 22$), which is a good polaron model compound of *trans*-PA. In this study, we also discuss to $TNBC^{\bullet-}$ as a polaron model have a long chain ($n = 22$) with $DP_n^{\bullet-}$ ($n = 4$, 6, 8, and 10) models. The chemical structures of the model compounds used in this study are schematically shown in Figure 1.

In this paper, we explain the difference of doping-induced Raman spectra between lightly and heavily Na-doped *trans*-PA. These spectra have also compared with those of the negatively charged soliton models (DP_3^-, DP_5^-, DP_7^-, DP_9^-, and DP_{13}^-) and the negatively charged polaron models ($DP_4^{\bullet-}$, $DP_6^{\bullet-}$, $DP_8^{\bullet-}$, $DP_{10}^{\bullet-}$, and $TNBC^{\bullet-}$; $n = 22$). The origin of the doping induced charged domains in *trans*-PA is discussed in terms of solitons and polarons.

Experimental Section

1. Materials. The cis-rich PA films prepared according to Shirakawa's method[26] at −78 °C were thermally isomerized to *trans*-PA films at 180 °C for 60 min. The *trans*-PA films were doped with Na by treating them with a solution of sodium naphthalide in THF in a completely sealed ampule.[14] Raman measurements were performed the film in the sealed ampule. The dopant concentration was controlled by both the concentration of sodium naphthalide and the period of immersing the film into the solution. Four kinds of Na-doped PA films were prepared under the various doping conditions. The Na concentration of the doped samples increases in order from sample I to sample IV. Here, we call samples I−II "lightly doped" and samples III−IV "heavily doped", respectively.

All α,ω-diphenylpolyenyl anions (DP_n^-, $n = 3$, 5, 7, 9, and 13) and their neutral species (DP_n) used in this experimental were synthesized by referring to the previous papers.[6,8] Li^+ prepared from *n*-butyllithium as a counterion was used. The charged species (DP_n^-) of DP_n were prepared in anhydrous THF solutions in a completely sealed quartz cell under high vacuum and were identified from the change of electronic absorption spectra. All-*trans*-1,4-diphenyl-1,3-tetradiene (DP_4), -*trans*-1,6-diphenyl-1,3,5-hexatriene (DP_6), -*trans*-1,8-diphenyl-1,3,5,7-octatetraene (DP_8), and -*trans*-1,10-diphenyl-1,3,5,7,9-decapentaene (DP_{10}) were purchased from the Tokyo Chemical Industry Co., Ltd., and Aldrich Chemical Co., Inc., respectively, and used without further purification. The radical anions ($DP_n^{\bullet-}$, $n = 4$, 6, 8, and 10) of each polyene were prepared by reduction of the neutral polyene with a sodium mirror in THF solution in a sealed glass ampule. This method was similar to that reported by Hoijtink and Meij.[27] The reduction reactions were followed by absorption spectroscopy. All-*trans*-19,19′,20,20′-tetranor-β,β-carotene (TNBC) and its radical anion ($TNBC^{\bullet-}$) were prepared as reported in our previous paper.[24]

The concentration of all samples was $10^{-5}\sim10^{-4}$ mol/dm^3 in THF in quartz cells (path length is 10 mm). Raman spectra were measured for such solutions in sealed cells.

2. Equipment. Raman spectra taken with the 1064 and 1320 nm laser line were measured on a JEOL JIR 5500 Fourier transform (FT) spectrophotometer modified for Raman measurements. A laser line was provided from a continuous-wave Nd:YAG laser (CVI YAG-MAX C-92). Then, the laser beam was passed through an interference filter to remove spontaneous emission lines and was led to the sample. The InGaAs and Ge detectors were used for Raman measurements with 1064 and 1320 nm excitations, respectively. Especially, for the 1320 nm laser line, the Raman scattered light was collected with a 90° off-axis parabolic mirror in a backscattering configuration and was passed through three long-wavelength-pass dielectric filters (Omega) to eliminate the Rayleigh scattered light. Raman measurements on this FT spectrophotometer were made at a spectral resolution of 4 cm^{-1}. Raman spectra excited with laser lines in the 488.0−753.0 nm region were measured at room temperature on a Raman spectrometer consisting of a Spex 1877 Triplemate and an EG & PARC 1421 intensified photodiode array detector. Several lines from a Coherent Radiation Innova 90 Ar ion laser (488.0 and 514.5 nm), a NEC GLG 108 He−Ne laser (632.8 nm), and a Spectra-Physics Model 375 dye laser (753.0 nm) were used for Raman excitation.

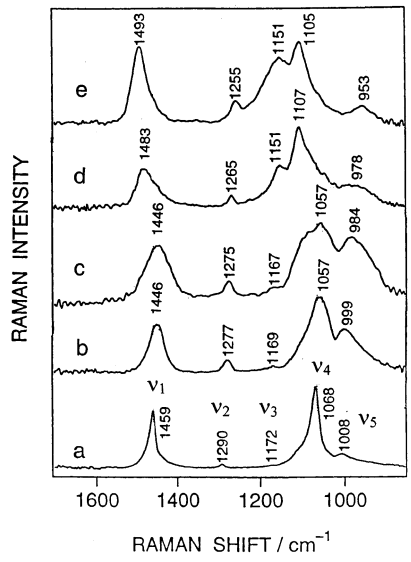

Figure 2. 1320 nm excited FT-Raman spectra of (a) pristine *trans*-PA, (b−c) lightly Na-doped PA, and (d−e) heavily Na-doped PA: (b) sample I, (c) sample II, (d) sample III, and (e) sample IV.

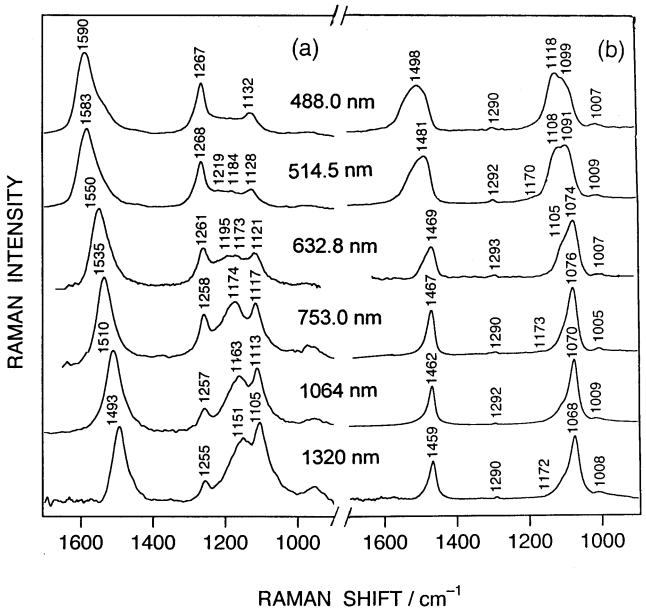

Figure 3. Raman spectra of heavily Na-doped *trans*-PA (sample IV) and its pristine. Excitation wavelengths are 1320, 1064, 753, 632.8, 514.5, and 488 nm for Na-doped *trans*-PA (a) and its pristine (b), respectively. Fluorescence backgrounds are subtracted from each spectrum. The Na content of sample IV is above 15 mol %.

Optical absorption spectra at various stages of the reduction process were measured on a Hitachi U-3500 spectrophotometer.

Results and Discussion

1. Raman Spectra of Lightly and Heavily Doped PA with Sodium. We showed the observed Raman spectra of lightly and heavily doped PA (in Figures 2 and 3a) and its pristine (Figure 3b), respectively. The Raman spectra of pristine *trans*-PA taken with several laser lines are shown in Figures 2a and 3b. In the 1320 nm excited Raman spectrum (Figure 2a), five bands are observed at 1459, 1290, 1172, 1068, and 1008 cm^{-1}, which we called ν_1, ν_2, ν_3, ν_4. and ν_5, respectively. The ν_1, ν_2, and ν_4 bands are undoubtedly assigned to Raman-active fundamentals[7−9] for an infinite planner polyene chain (C_{2h} symmetry). The ν_3 band was attributed to the $\delta = \pi$ mode (where δ is the phase difference between the adjacent −CH═CH− units) of the ν_4 branch,[28] in which neighboring −CH═CH− units move in opposite directions. The Raman bands corresponding to ν_1, ν_2, ν_3, and ν_4 are observed for α,ω-di-*tert*-butylpolyenes,[29] although the Raman band corresponding to ν_3 is not observed for unsubstituted polyenes. The ν_5 band was attributed to the in-phase ($\delta = 0$) CH out-of-plane bending on the basis of the frequency shifts of ^{13}C and ^{2}H substitutions.[28] The ν_3 and ν_5 bands, which are Raman-inactive for an infinite planer chain, probably appear in the Raman spectrum because of symmetry lowering due to distortion of the polyene chain. Tasumi et al.[30] have pointed out that the in-phase CH out-of-plane bending mode appears in the Raman spectra of some carotenoids due to distortion of the polyene chain.

The Raman spectra of Na-doped PA taken with the 1320 nm laser line are shown in Figure 2b−e. The Na concentration increases from spectrum b to e in Figure 2, although the Na concentrations are not precisely determined in the present study. In our previous paper,[31] we reported the Raman spectra of *trans*-PA doped with Na at various concentrations. From those results, we call samples I−II "lightly doped" (doping level is below 6 mol %) and samples III−IV "heavily doped" (doping level is above 11 mol %), respectively.

The 1320-nm excited Raman spectra of lightly doped samples (Figure 2 parts b and c) show small but significant spectral changes with increasing Na concentration. The spectral characteristics are as follows. For the ν_1 band, a shoulder or a peak is observed at 1446 cm^{-1}. This wavenumber position is lower than that at 1459 cm^{-1} for pristine *trans*-PA (Figure 2a). The ν_2 band is observed between 1277 and 1275 cm^{-1}. These low wavenumber positions for the ν_2 band are characteristic of negatively charged polyenes.[15] The ν_3 band is weak in intensity between 1169 and 1167 cm^{-1} and shows small downshifts with increasing Na concentration. For the ν_4 band, a broad or a peak is observed at 1057 cm^{-1}. This wavenumber position is lower than that at 1068 cm^{-1} for pristine *trans*-PA (Figure 2a). In Figure 2c, the shoulder band of ν_4 peak (1057 cm^{-1}) strongly showed on its higher energy side (1100−1107 cm^{-1}), and the width of ν_4 band with ν_1 band also becomes more broad dispersion. Here, the narrow or broad of band shape, especially in the ν_1 and ν_4 bands (C═C and C−C stretches), relates with distribution range of charged domains in doped PA. This shoulder band of ν_4 is also increased with doping level increase, and in the step of highly doping (Figure 2 parts d and e), this band becomes to the main band instead of 1057 cm^{-1} band of lightly doping (Figure 2 parts b and c). Accordingly, in the case of Figure 2c, we think that the some domains of highly doped PA (so-called polaron lattice structure) are in a lightly doped PA sample. Kivelson and Heeger[32] have proposed that the charged species in heavily doped PA are a polaron lattice structure. The ν_5 band undergoes downshifts, and its intensity increases markedly, as the Na concentration increases. The strong intensity of the ν_5 band may arise from the mixing of the CH out-of-plane bending mode with the CC stretching modes due to the distortion of charges domains in the polyene chain. When *trans*-PA is doped with sodium, negative solitons or negative polarons are expected to form. A soliton has C_{2v} local symmetry, whereas a polaron has C_{2h} local symmetry. In the Raman studies of lightly Na-doped *trans*-PA, doping-induced Raman bands associated with charged domains generated by doping were observed for the first time by the 1320 nm line. It seems therefore probable that the observed doping-induced Raman bands are due to negative solitons. Experimental results for lightly Na-doped *trans*-PA obtained by electronic spin

resonance spectroscopy have been explained in terms of negative solitons generated by Na doping.[1]

The 1320-nm excited Raman spectra of heavily doped samples (Figure 2 parts d and e) are quite different from those of lightly doped *trans*-PA. The peaks of the ν_1 band are observed in a higher wavenumber region (between 1483 and 1493 cm^{-1}) in comparison with those of pristine and lightly doped *trans*-PA. Here, the shape of the ν_1 band in Figure 2d is broader than that of Figure 2e and the shoulder of ν_1 band in Figure 2d shows on its low energy side, and this shoulder band is gone at a higher doping level (Figure 2e), and the width of the band is also more narrowing. Accordingly, in the case of Figure 2d, we consider that some domains of lightly doped PA (so-called soliton lattice structure) are in a highly doped PA. The ν_2 band shows further downshifts with increasing Na concentration. The ν_3 band is observed at 1151 cm^{-1}, and its intensity increases greatly with increasing Na concentration. It should be noted that this band corresponds to the $\delta = \pi$ mode of the pristine *trans*-PA. The peaks observed between 1107 and 1105 cm^{-1} are attributed to the ν_4 band. These observed wavenumbers of the ν_4 band are higher than those of pristine and lightly doped *trans*-PAs. The ν_5 band shifts downward, and its intensity decreases. Thus, the doping-induced Raman bands of heavily Na-doped *trans*-PA are clearly different from those of lightly Na-doped *trans*-PA (Figure 2 parts b and c).

The Raman spectra of the fully Na-doped *trans*-PA (sample IV) and its pristine film measured with several excitation wavelengths between 488.0 and 1320 nm (between 2.54 and 0.94 eV) are shown in Figure 3 parts a and b, respectively. The 632.8 nm excited Raman spectrum in Figure 3a is similar to that of $CHNa_{0.17}$ reported by Eckhardt et al.[12] and those of $CHNa_{0.15}$ reported by Tanaka et al.[13] These similarities indicate that the Na content of our sample IV is not less than 15 mol %.

A strong band (ν_1 band) is observed between 1493 and 1590 cm^{-1}. This ν_1 band group shifts upward with decreasing excitation wavelength: 1493, 1510, 1535, 1550, and 1590 cm^{-1} for the 1320, 1064, 753, 632.8, and 488 nm laser lines, respectively. The ν_2 band group is observed between 1255 and 1267 cm^{-1}. The wavenumber of these bands are intensive to excitation wavelength, whereas the relative intensity increases with decreasing excitation wavelength. A broad ν_3 band is observed in the range between 1151 and 1173 cm^{-1}, except for the 488 nm excited spectrum. The band in this group also shifts upward, as the excitation wavelength becomes shorter. A ν_4 band is observed between 1105 and 1132 cm^{-1}. The band in this group also shifts upward, but its relative intensity decreases with decreasing excitation wavelength.

The above features of the Raman spectra of Na-doped PA will be compared with those of the soliton and polaron models in the following section. In particular, the large wavenumber range observed for the ν_1 band will be explained by the existence of charge domains with various localization lengths.

2. Raman Spectra of Soliton and Polaron Model Compounds. The 1064 nm excited FT-Raman spectra of the negatively charged soliton models (DP_3^-, DP_5^-, DP_7^-, DP_9^-, and DP_{13}^-) in the THF solutions are shown in Figure 4. It was not possible to observe a resonant Raman spectrum within the electronic absorption regions, because of the presence of an intense fluorescent background. The Raman spectra of the negatively charged soliton models, however, could be obtained with excitation at 1064 nm (1.17 eV). The 1064 nm laser line is located more at the low-energy side than the electronic absorption energies of DP_n^- (DP_3^-, 2.21 eV; DP_5^-, 2.07 eV; DP_7^-, 1.91 eV; DP_9^-, 1.76 eV; DP_{13}^-, 1.52 eV, respectively).

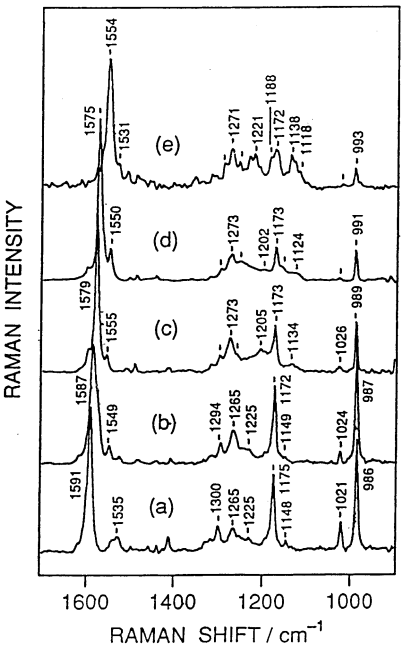

Figure 4. 1064 nm excited FT-Raman spectra of (a) DP_3^-, (b) DP_5^-, (c) DP_7^-, (d) DP_9^-, and (e) DP_{13}^- in THF solutions, respectively. Bands due to THF and backgrounds are subtracted in all spectra.

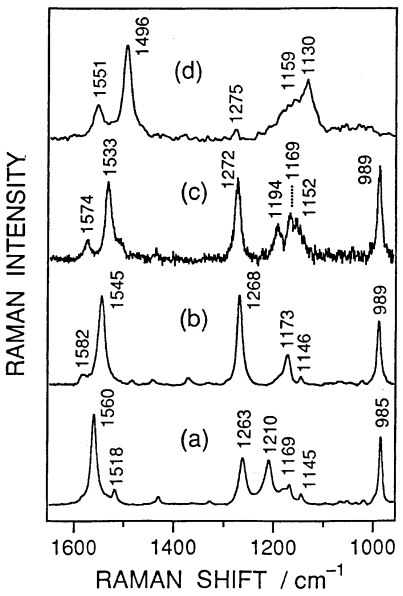

Figure 5. Raman spectra of (a) $DP_6^{\bullet-}$, (b) $DP_8^{\bullet-}$, (c) $DP_{10}^{\bullet-}$, and (d) $TNBC^{\bullet-}$ in THF solutions. Excitation wavelengths are 632.8, 632.8, 753, and 1064 nm for a−d, respectively. Fluorescence backgrounds are subtracted in all spectra.

Raman spectra of the negatively charged polaron models ($DP_6^{\bullet-}$, $DP_8^{\bullet-}$, $DP_{10}^{\bullet-}$, and $TNBC^{\bullet-}$; $n = 22$) with in the THF solutions are shown in Figure 5. The excitation wavelengths are 632.8, 632.8, 753, and 1064 nm for $DP_6^{\bullet-}$, $DP_8^{\bullet-}$, $DP_{10}^{\bullet-}$, and $TNBC^{\bullet-}$, respectively. The four characteristic band features observed by the present results are summarized as follows.

(1) ν_1 Band. A strong band, which is assignable to the C═C stretching vibration, is observed at the 1591 (DP_3^-), 1587 (DP_5^-), 1579 (DP_7^-), 1575 (DP_9^-), and 1554 cm^{-1} (DP_{13}^-), for soliton models, respectively. This band shifts downward as the *n* number increases from 3 to 13. These wavenumbers of C═C stretching band are slightly higher than those of the corresponding bands of neutral polyenes (DP_n; *n* is an even number): 1576 (DP_8) and 1557 cm^{-1} (DP_{10}), whereas the

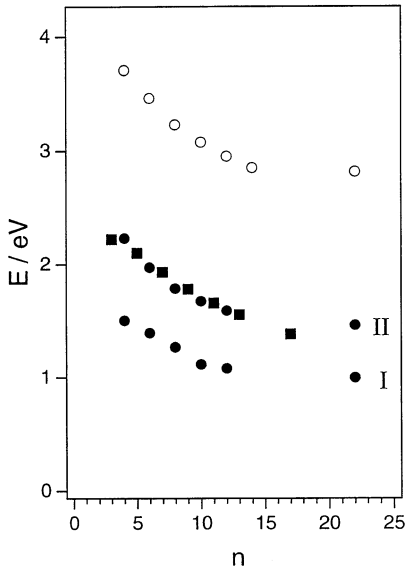

Figure 6. Relationship between *n* and observed electronic transition energies (*E*). ○, DP_n and TNBC; ■, DP_n-; ●, $DP_n^{\bullet-}$ and $TNBC^{\bullet-}$.

contrary is the case for the radical anions "polaron model": 1560 ($DP_6^{\bullet-}$), 1545 ($DP_8^{\bullet-}$), 1533 ($DP_{10}^{\bullet-}$), and 1496 cm^{-1} ($TNBC^{\bullet-}$), of Figure 5. In particular, the 1496 cm^{-1} peak position of $TNBC^{\bullet-}$ (in Figure 5d) is very similar to the ν_1 band (1493 cm^{-1}) position of the heavily doped PA with sodium excited at 1320 nm laser line (in Figure 3a), this result also indicate that the localized carbon number (*n*) in the charged domains of doped PA excited at 1320 nm laser line is about 22 and that the doping induced charged domain in heavily doped PA can be discussed in terms of a polaron.

In Figure 6, we showed the relationship between *n* and observed ν_1 frequencies. On the other hand, it indicates that the bond orders or the bond alternations in the anions (soliton) are different from not only their neutrals but also in the radical anion species (polaron). Especially, the lower wavenumber shift of each C═C stretching band in the radical anions reflects a decrease in the C═C bond order, which suggests a change in regular bond alteration. According to the ab initio molecular orbital calculations of the radical cations of 1,3-butadiene to 1,3,5,7,9-decapentaene reported by Kawashima et al.,[25] bond alternation disappears at the center of the chain of each radical cation. The present observation suggests that a similar change in bond alteration also occurs in the case of the radical anions.

(2) ν_2 Band. In both soliton and polaron models, this band was observed between 1263 and 1277 cm^{-1} and can be assigned to the CH in-plane bend. These wavenumbers of ν_2 band are located lower about 10−15 cm^{-1} than those of neutral polyenes. The change of wavenumbers with increasing *n* is very small, but it corresponds well to the ν_2 band of doped PA. In the case of dianion model (bipolaron), the ν_2 band is observed at the same position as that of the radical anions or anions. Thus, the position of the ν_2 band may be a marker of the negatively charged polyenes or donor doped PA. However, in the case of polaron models, the relatively intensity of ν_2 band in $TNBC^{\bullet-}$ model be remarkably weaker than those of $DP_n^{\bullet-}$ (n = 6, 8, and 10). On the contrary, the relatively intensity of ν_2 band shows no changes in soliton models.

(3) ν_3 , ν_4, and ν_5 Bands. Two or three peaks for the ν_3 and ν_4 bands are observed in the range between 1210 and 1110 cm^{-1}. These ν_3 and ν_4 bands can be assigned to the mixing band between C−C and C═C stretches.[24] Especially, the relatively intensity of ν_3 and ν_4 bands in $TNBC^{\bullet-}$ model is correspondingly stronger than those of $DP_n^{\bullet-}$ (n = 6, 8, and 10), whereas the contrary is the case for the ν_2 band as described previously. However, in the case of soliton models, the relatively intensity of ν_3 and ν_4 bands show no change. However, in polaron models, these spectrum patterns of ν_3 and ν_4 bands with the as described above ν_2 band are very similar to that of the Raman spectra of the heavily doped PA measured with several excitation wavelengths between 488.0 and 1320 nm as show in Figure 3a. These results indicate that the segments of charged domain having various conjugation lengths exist in doped PA.

The ν_5 band (CH out-of plan) measured in doped PA could not be observed at the model compounds. In the wavenumber region above 1000 cm^{-1} in the Raman spectra of the ionic species, the phenyl-group modes are not strongly observed except for a strong band in the region between 1172 and 1173 cm^{-1}. In particular, the effect of phenyl groups decreases with the *n* increase. Thus, these ionic species are suitable as models of negatively charged soliton or negative polaron in *trans*-PA.

3. Self-Localized Excitations in Sodium-Doped PA. The large dispersion (1590∼1493 cm^{-1}) of the ν_1 bands (Figure 3a) according to the exchange of excitation laser line (488.0∼1320 nm) and excitation photon energies (2.54 ∼ 0.94 eV) can be also explained as the existence of charged domains with various localization lengths. These charged domains have respectively different electronic absorptions, and the Raman bands arising from a domain are resonantly enhanced when the wavelength of the excitation laser line is located within the electronic absorption of the same domain. Thus, in this section, we discuss the relationship between the electronic transition energies (E/eV) of the soliton (DP_n^-) and polaron model compounds ($DP_n^{\bullet-}$ and $TNBC^{\bullet-}$) and the ν_1 Raman frequencies and the relationship between the excitation photon energies (E_{ex}/eV) of doped PA and the ν_1 Raman frequencies.

In Figure 6, we have plotted the relationship *n* of the model compounds and its observed electronic transition energies (E/eV), respectively. In soliton models (DP_n^-), all spectra have an absorption containing a single strong peak attributed the $n-\pi^*$ transition, and these peaks shifted to lower energies with increasing the carbon numbers (*n*) of the polyene part. Thus, in the MO energy levels of a soliton model with odd numbered carbons, a nonbonding energy level, which is occupied by two electrons, is formed in the center of the band gap. According to the theory using a continuum model, a soliton in PA is expected to give rise to one peak at the mid-gap center (0.5−0.9 eV). In polaron models ($DP_n^{\bullet-}$ and $TNBC^{\bullet-}$), a strong absorption peak and a weak peak are apparently attributed the $1^2B_g \rightarrow 2^2A_u$ and $1^2B_g \rightarrow 1^2A_u$ transitions (π-π^*), respectively.[25] These two absorption peaks have been attributed to the two allowed transitions on the basis of the results of semiempirical self-consistent-field calculations combined with a limited configuration interaction.[33] The lower energy band (I) is very weak, and the higher band (II) has a strong absorption peak. According to a theoretical calculation[34] using a continuum model, a negative polaron in PA is expected to give rise to two strong bands (ω_1, antibonding level → conduction band; ω_2, bonding level → antibonding level). The observed bands (I and II) of the polaron models correspond to the ω_1 and ω_2 bands, respectively, though the intensity of band I is weak. However, the ω_3 transition was symmetry forbidden.

As shown in section 2, the Raman spectra of the negatively charged soliton models and the negative polaron models are very similar to their spectrum patterns as a whole, but their wavenumbers and relative intensities are mutually different to

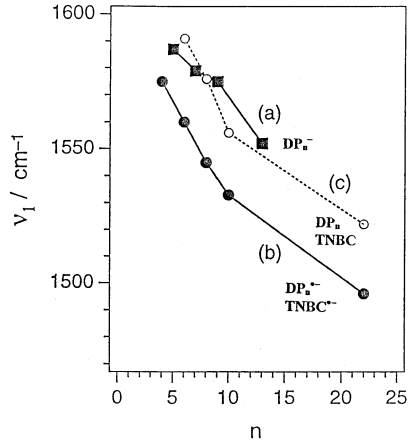

Figure 7. Relationship between n and ν_1 frequencies. (a) DP_n^-; (b) $DP_n^{\bullet-}$ and $TNBC^{\bullet-}$; (c) DP_n and TNBC.

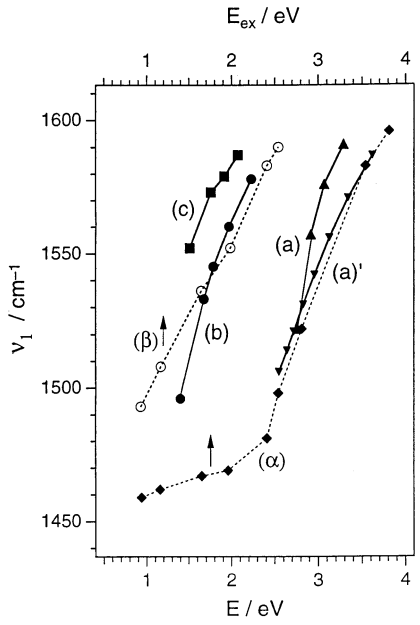

Figure 8. Relationships between excitation photon energies (E_{ex}/eV) for polymer and electronic transition energies (E/eV) for model compounds and ν_1 Raman frequencies. (α) pristine *trans*-PA; (β) heavily Na-doped PA; (a) DP_n and TNBC; (a′) dibutylpolyenes (ref 29); (b) $DP_n^{\bullet-}$ and $TNBC^{\bullet-}$; (c) DP_n^-.

some extent. Thus, as shown in Figure 7, the wavenumbers of the ν_1 band, both the negatively charged soliton models and the negative polaron models, shift downward according to n. However, the ν_1 wavenumbers of the negatively charged soliton are higher than those of the negative polaron. In Figure 8, we have plotted the ν_1 wavenumbers of model compounds against the electronic transition energies (E/eV), neutral polyene (a and a′), negative polaron models (b), and negatively charged soliton models (c), respectively. The ν_1 wavenumber of the model compounds is higher with increasing electronic transition energies (decreasing conjugation lengths). As shown in Figure 7, the ν_1 band is sensitive to the conjugation lengths (electronic transition energies); thus, this band shows a drastic decrease in wavenumber as the conjugation lengths increase. We have also plotted the ν_1 Raman wavenumbers of *trans*-PA against the Raman excitation photon energies (E_{ex}/eV), pristine PA (Figure 8α), and heavily Na-doped −PA (Figure 8β), respectively. The data of pristine PA (Figure 8α) are very similar with that of neutral polyene models (Figure 8 parts a and a′), and the data of heavily Na-doped PA (Figure 8-â) are vary similar with that of charged model species (Figure 8 parts b and c), especially, polaron models (Figure 8b). From these results, the self-localized excitation states in doping induced PA can be interpreted as the distribution of the charged domains having various localization lengths; thus, this large Raman frequency dispersion in the heavily Na-doped PA had been selectively observed by the resonance Raman effects. However, at the same Raman excitation photon energies (E_{ex}/eV), ν_1 wavenumbers of doped-PA had been observed at higher wavenumbers than those of pristine PA at the same Raman excitation photon energies (E_{ex}/eV) as shown in Figure 8 parts α and β. It can be interpreted that the ν_1 wavenumbers of self-localized excitation states are higher than those of the neutral polymer having electronic absorption at the same position. We also suggest that the localized carbon number (n) in the charged domains of heavily doped PA can be distributed until about 4−22 from comparing with ν_1 wavenumbers of polaron models ($n = 4 \sim 22$) and those of lightly doped PA until at least 33−37 from extension of chain lengths for soliton models ($n = 3 \sim 13$), respectively. However, studies of the Raman spectra of longer soliton model compounds are a requisite for further elucidation of the self-localized charge domains in PA.

Summary

Raman spectra obtained from heavily doped *trans*-PA are quite different from those of lightly doped trans-PA. In the wavenumber region above 1000 cm^{-1}of the Raman spectrum of PA, five groups of bands have been observed. These spectra have also been compared with those of the negatively charged soliton models (DP_n^-) and the negatively charged polaron models ($DP_n^{\bullet-}$ and $TNBC^{\bullet-}$). Raman spectra of soliton models (DP_n^-) were observed for the first time. The difference between Raman spectra of the negatively charged soliton models and the negative polaron models are also explained with those of doped PA. Especially, the Raman spectra of heavily Na-doped PA were very similar with those of polaron models. The large wavenumber dispersion observed for the ν_1 bands in Na-doped *trans*-PA can be explained by the existence of the charged domains with various localization lengths. In particular, the position of the ν_1 band (1493 cm^{-1}) of Na-doped *trans*-PA with 1320 nm laser line is observed at a very similar position (1496 cm^{-1}) with the radical anion of TNBC containing eleven conjugated C═C bonds. This similarity indicates that the charged domains generated by Na-doping in the polymer chain are localized over eleven conjugated C═C bonds.

References and Notes

(1) Heeger, A. J.; Kivelson, S.; Schrieffer, J. R.; Su, W.-P. *Rev. Mod. Phys.* **1988**, *60*, 781.

(2) Kiess, H. G., Ed.; *Conjugated Conducting Polymers*; Springer: Berlin, 1992.

(3) Shirakawa, H.; Louis, E. J.; MacDiarmid, A. G.; Chiang, C. K.; Heeger, A. J. *J. Chem. Soc., Chem. Commun.* **1977**, 578.

(4) Chung, T.-C.; Moraes, F.; Flood, J. D.; Heeger, A. J. *Phys. Rev. B* **1984**, *29*, 2341.

(5) Heeger, A. J.; Kivelson, S.; Schrieffer, J. R.; Su, W.-P. *Rev. Mod. Phys.* **1988**, *60*, 781.

(6) Ikehata, S.; Kaufer, J.; Woerner, T.; Pron, A.; Druy, M. A.; Sivak, A.; Heeger, A. J.; MacDiarmid, A. G. *Phys. Rev. Lett.* **1980**, *45*, 1123.

(7) Kuzmany, H. *Macromol. Chem., Macromol. Symp.* **1990**, *37*, 81.

(8) Harada, I.; Furukawa, Y. In *Vibrational Spectra and Structure*; Durig, J. R., Ed.; Elsevier: Amsterdam, 1991; Vol. 19, p 369.

(9) Gussoni, M.; Castiglioni, C.; Zerbi, G. In *Spectroscopy of Advanced Materials*; Clark, R. J. H., Hester, R. E., Eds.; Wiley: Chichester, U.K., 1991; p 251.

(10) Furukawa, Y.; Harada, I.; Tasumi, M.; Shirakawa, H.; Ikeda, S. *Chem. Lett.* **1981**, 1489.

(11) Faulques, E.; Lefrant, S.; Rachdi, F.; Bernier, P. *Synth. Met.* **1984**, *9*, 53.

(12) Eckhardt, H.; Shacklette, L. W.; Szobota, J. S.; Baughman, R. H. *Mol. Cryst. Liq. Cryst.* **1985**, *117*, 401.
(13) Tanaka, J.; Saito, Y.; Shimizu, M.; Tanaka, C.; Tanaka, M. *Bull. Chem. Soc. Jpn.* **1987**, *60*, 1595.
(14) Furukawa, Y.; Ohta, H.; Sakamoto, A.; Tasumi, M. *Spectrochim. Acta* **1991**, *47A*, 1367.
(15) Furukawa, Y.; Uchida, Y.; Tasumi, M.; Spangler, C. W. *Mol. Cryst. Liq. Cryst.* **1994**, *256*, 721.
(16) Lefrant, S.; Mulazzi, E.; Mathis, C. *Phys. Rev. B* **1994**, *49*, 13400.
(17) Furukawa, Y. *J. Phys. Chem.* **1996**, *100*, 15644.
(18) Bally, T.; Heilbronner, E. In *The Chemistry of Dienes and Polyenes*; Rappoport, Ed.; Wiley: Chichester, U.K., 1997; Vol. 1, pp 173−261.
(19) Tolbert, L. M.; Ogle, E. *J. Am. Chem. Soc.* **1989**, *111*, 5959; *Synth. Met.* **1991**, *41*, 1389.
(20) Spangler, C. W.; Liu, P.-K.; Dembek, A. A.; Havelka, K. O. *J. Chem. Soc., Perkin Trans.* **1991**, *1*, 799.
(21) Furukawa, Y.; Sakamoto, A.; Ohta, H.; Tasumi, M. *Synth. Met.* **1992**, *49*, 335.
(22) Ehrenfreund, E.; Moses, D.; Heeger, A. J.; Cornil, J.; Bredas, J. L. *Chem. Phys. Lett.* **1992**, *196*, 84.
(23) Bally, T.; Roth, K.; Tang, W.; Schrock, R. R.; Knoll, K.; Park, L. Y. *J. Am. Chem. Soc.* **1992**, *114*, 2440.
(24) Kim, J. Y.; Furukawa, Y.; Tasumi, M. *Chem. Phys. Lett.* **1997**, *276*, 418.
(25) Kawashima, Y.; Nakayama, K.; Nakano, H.; Hirano, K. *Chem. Phys. Lett.* **1997**, *267*, 82.
(26) Ito, T.; Shirakawa, H.; Ikeda, S. *J. Polym. Sci. Polym. Chem. Ed.* **1974**, *12*, 11.
(27) Hoijtink, G. J.; Von der Meij, P. H. *Zert. Phys. Chem. Neue. Folge*. **1959**, *20*, 1.
(28) Takeuchi, H.; Arakawa, T.; Furukawa, Y.; Harada, I.; Shirakawa, H. *J. Mol. Struct.* **1987**, *158*, 179.
(29) Schaffer, H. E.; Chance, R. R.; Silbey, R. J.; Knoll, K.; Schrock, R. R. *J. Chem. Phys.* **1991**, *94*, 4161.
(30) Hayashi, H.; Noguchi, T.; Tasumi, M. *Photochem. Photobiol*. **1989**, *49*, 337.
(31) Kim, J. Y.; Ando, S.; Sakamoto, A.; Furukawa, Y.; Tasumi, M. *Synth. Met.* **1997**, *89*, 149.
(32) Kivelson, S.; Heeger, A. J. *Phys. Rev. Lett.* **1985**, *55*, 308.
(33) Zahradník, R.; Cársky, P. *J. Phys. Chem.* **1970**, *74*, 1240.
(34) Fesser, K.; Bishop, A. R.; Campbell, D. K. *Phys. Rev. B* **1983**, *27*, 4804.